Adiabatic stabilization against photoionization: An experimental study

M. P. de Boer, J. H. Hoogenraad, R. B. Vrijen, R. C. Constantinescu, L. D. Noordam, and H. G. Muller
FOM–Institute for Atomic and Molecular Physics, Kruislaan 407, 1098 SJ Amsterdam, The Netherlands
(Received 19 January 1994)

We describe a detailed account of an experiment demonstrating light-induced stabilization against photoionization. The choice of initial state and atom is discussed in relation to the laser wavelength and laser pulse duration. In combination with a 100-fs, 620-nm probe pulse, the optimum choice is the circular 5*g* state in neon. A picosecond pump laser was used to prepare this Rydberg state. Initially, the population in this state was probed with a nanosecond laser pulse. Subsequently, the nanosecond probe pulse was replaced by an intense, (sub)picosecond pulse and the photoionization signal was studied. When the probe intensity is several times 10^{13} W/cm^2 a decrease in yield with respect to a less intense pulse with the same fluence is observed, which indicates stabilization. The results are in accordance with recent theoretical predictions.

PACS number(s): 32.80.Rm, 42.50.Hz

I. OVERVIEW

Since the invention of the laser, photoionization studies on atoms have been performed at ever increasing intensities. Numerous aspects of high-intensity photoionization could be accounted for by using elementary theories such as lowest-order perturbation theory (LOPT), over-the-barrier ionization, or quantum tunneling theory [1]. LOPT, however, cannot account for an effect such as above threshold ionization (ATI). Recent theories do account for light intensities around 1 a.u. (3.5×10^{16} W/cm^2) [2], with several groups working on nonperturbative approaches to the calculation of photoionization.

High-frequency theory is an example of such a nonperturbative theory [3]. In this theory the expansion parameter is not the intensity of the light field but rather the inverse frequency. The zero-order approximation is that the light frequency is infinitely high and successive approximations can be made by including more orders of the inverse frequency.

One of the predictions of high-frequency theory is an effect called stabilization [4]. In the calculations the ionization rate decreases once the intensity rises above a critical intensity. This very counterintuitive prediction was originally made for the ground state of atomic hydrogen subjected to high-energy photons at intensities in excess of 1 a.u.

This paper describes in detail experimental evidence for stabilization [5]. In Sec. II we discuss the physical mechanism that is responsible for stabilization and we distinguish two possible kinds. High-lying Rydberg states also show stabilization and are experimentally much more feasible, as discussed in Sec. III. A detailed account of the considerations that eventually led to the actual experimental configuration is given in Sec. IV. Section V describes the experimental preparation of the 5*g* Rydberg state, while Sec. VI describes the ionization step that actually demonstrated stabilization.

II. INTRODUCTION

A. Photoionization at low intensities

For low intensities the theory of photoionization is well developed. It was initiated by Einstein's explanation in 1905 of the photoelectric effect [6]. If the photon energy of the ionizing radiation is high enough, there is a finite probability for a photon to be absorbed. The energy of the photon is partly used to overcome the ionization threshold and the excess energy is transformed into kinetic energy of the emitted electron.

The ionization rate Γ of an atom can be calculated using Fermi's "golden rule" [7]:

$$\Gamma=4\pi^2/h\,|\langle f|H|i\rangle|^2\rho(E_k)\,, \tag{1}$$

where $|i\rangle$ is the initial state, $|f\rangle$ the final state, and $\rho(E_k)$ the density of states in the continuum, at the energy of the emitted electron.

Since the interaction Hamiltonian H is proportional to the electric-field strength, the ionization rate increases with intensity and depends linearly on the flux of photons. The total ionization yield depends on the fluence (time-integrated intensity). A trivial exception to the linear dependence on intensity is depletion of initial-state atoms. Fermi's "golden rule" also no longer applies if resonances play a role. In this paper we are concerned with single-photon ionization, where resonances do not play a role as long as there is no structure in the continuum.

B. Adiabatic stabilization

Once the intensity passes a certain critical threshold, the single-photon ionization rate no longer follows Fermi's "golden rule," but actually decreases with increasing intensity. This effect is called *adiabatic* stabilization, because the stabilized state is reached by adiabatic

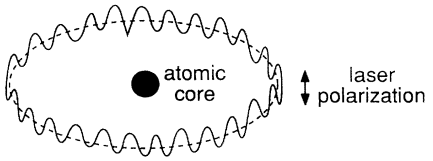

FIG. 1. A quivering electron on a classical trajectory. Quantum mechanically, the wave function is spread out over the classical trajectory and oscillates along with the electric field of the laser.

evolution of the initial state. Transitions to other bound states do not play a role in this process, so that it can occur for an isolated initial state. The suppression is not temporary but lasts as long as the intensity is high.

The essence of adiabatic stabilization is that the high intensity distorts the initial electron wave function, and this can be visualized easily (see Fig. 1): Subjecting the atom to an intense laser field results in an electromagnetic force on the electron that is large compared to the force binding the electron to the nucleus. The electromagnetic force shakes the electron wave function in the direction of laser polarization and results in a quiver motion. This quiver motion itself is periodic, and therefore does not cause any ionization. This can be most easily seen when we transform the reference frame to a coordinate system that moves along with a freely quivering electron (Kramers-Henneberger frame [8]). In the new frame it is the nucleus which oscillates, while the wave function of a free electron does not. A bound electron quivers like a free one if the light frequency is high compared to that of the orbital motion. Due to the oscillating nucleus, the wave function will undergo a time-varying force which can cause ionization. The time-averaged part of the force binds the electron and will not contribute any ionization. At small quiver amplitudes the time-varying force varies harmonically and is proportional to the light intensity. This is the regime where ionization is well described by perturbative theories.

Once the quiver amplitude is much larger than the initial wave function, however, the wave function will see the nucleus racing by every so often, but for most of the time the electron will be far away from the nucleus and feel hardly any force. The peak force, at the point of minimum separation, will saturate but the duration of that force will keep going down. As a result, the time-averaged force will decrease with intensity as well as the total power of the time-varying components. This will result in a decrease of the ionization rate. The effect actually contains a positive feedback loop: Once the time-averaged force decreases, the electron will be bound more weakly. This means that the wave function will be located further from the nucleus and so both the peak force and time-averaged force will decrease even further. This leads to a very rapid increase of the lifetime with intensity as soon as the critical intensity is exceeded (see Fig. 2).

C. Competing stabilization mechanisms

Adiabatic stabilization is not the only mechanism that can suppress photoionization at high intensities. Transient stabilization [9] is another notable exception to Fermi's "golden rule." It refers to a temporary suppression of the photoionization yield, an effect which has recently been demonstrated [10].

The most intuitive description of transient stabilization is in the time domain: Transient stabilization can occur if a Rydberg state is photoionized by a pulse much shorter than the classical round-trip time of the electron. Since photoionization occurs near the core [11,12], the wave function can become depleted there, while the wave function far away from the core has no time to reach it and is therefore not able to absorb photons. Increasing the intensity will hardly increase the yield, once depletion of the wave function near the core has set in. The yield can only increase if the pulse is made longer, rather than more intense. For a longer pulse the outer part of the wave function has time to reach the core and contribute to the photoionization yield.

There is an equivalent description in the frequency domain: The high intensity causes the depletion of the initial state. Apart from photoionization, there is also a transfer of population to nearby Rydberg states that lie within the bandwidth of the laser pulse. The coherent superposition of these neighboring states causes the wave function to develop a hole or notch (antiwave packet) near the core. Ionization from the populated neighboring states interferes destructively with the ionization from the initial state and hence the photoionization yield decreases.

In a variation on this theme the ionization is also suppressed due to interference between neighboring states. In this case of so-called interference stabilization [13], however, the neighboring states are populated, not due to the large laser bandwidth, but due to the large lifetime broadening of the excited states. In our experiments, the conditions are chosen such that transient stabilization can be ruled out, since the spacing of the states is relatively large. In this way we ensure that any stabilization we observe is of the adiabatic type.

A steep decrease in ionization rate with intensity can also occur as a result of Stark shifts, either of resonant bound states [14] or the continuum threshold [15] ("resonance stabilization" [16]). In our experiment, conducted in the short-pulse regime [17], channel closure would reveal itself by the accompanying shift of the photoelectron energy towards (and eventually beyond) zero. The appearance of sharply defined electron energies thus constitutes proof that channel closure does not occur.

III. ADIABATIC STABILIZATION OF RYDBERG STATES

A. Rydberg states versus ground-state atomic hydrogen

Pont and Gavrila [4] first predicted that the ground state of atomic hydrogen, irradiated with high-frequency light, should show adiabatic stabilization at sufficiently high intensities. This prediction was later confirmed through the use of other numerical methods [18]. All these methods employed quantum-mechanical calculations describing atomic hydrogen in the ground state.

These calculations showed that an experiment showing stabilization would depend on three requirements being fulfilled simultaneously: First, a single photon should have sufficient energy to photoionize the atom ($h\nu > 13.6$ eV). Second, to prevent ionization of all the atoms during the leading edge of the pulse, the pulse duration should be shorter than a few femtoseconds. In the third place, the intensity should be around the critical intensity of 1 a.u. (3.5×10^{16} W/cm^2). To date, there is no light source that fulfills even two of these conditions.

Stabilization is not limited to ground-state hydrogen, however. Calculations have been performed for Rydberg states [19,20] that predict stabilization under more favorable experimental circumstances ($h\nu=2$ eV, $I_{cr}=5\times10^{13}$ W/cm^2, $t<500$ fs).

B. The high-frequency condition

If the frequency of the electromagnetic field is high enough, a bound electron will quiver in this field as though it were free. Figure 1 shows a quivering electron on a classical orbit. Stabilization can only occur if the electron wave function is not able to respond to the time-varying electromagnetic field within one optical cycle. The response time of the electron is determined by the classical round-trip time. In practical terms this means that the photon energy should be much higher than the ionization energy of the ground state. This requirement is called the high-frequency condition.

The response time of the electron cloud is not only determined by the initial state of the atom but also by the response time of any state to which the initial state can couple. Of all the Rydberg states within one n manifold, the circular state is the one with maximum l and m quantum numbers ($l=m=n-1$). If we try to ionize such a state with linearly polarized light, it mimics a ground state in that it only couples to higher-lying states, since selection rules ($\Delta m=0$) only allow coupling to states with the same m quantum number. This means that if the photon energy is larger than the binding energy of the initial state, then it will also be larger than the binding energy of any state to which it can couple. Therefore, it is best to use circular Rydberg states to fulfill the high-frequency condition.

C. "Death Valley"

Observing high-intensity effects can be prevented by the Death Valley problem, i.e., ionization of all atoms before the peak intensity is reached [21]. The dependence of the lifetime versus intensity can be classified into three regimes, as sketched in Fig. 2: At low intensities the lifetime behaves perturbatively and decreases according to Eq. (1) as the inverse of the intensity. This regime is characterized by a straight line with a slope of -1 in a log-log plot. At high intensities the stabilization regime is reached where the lifetime actually increases with intensity. In the intermediate regime around the critical intensity (Death Valley region), there is a minimum in the lifetime.

Death Valley poses a problem, since in a real experiment an atom will be subjected to a range of intensities. The intensity starts from zero, increases to some peak intensity, and then decreases back to zero again. To reach the stabilization regime, the atom must remain unionized during the rising edge of the pulse, i.e., the minimum lifetime must be at least of the order of the rise time. A pulse with sharp edges is therefore a critical requirement for an appreciable survival probability. In addition, the minimum lifetime should be long.

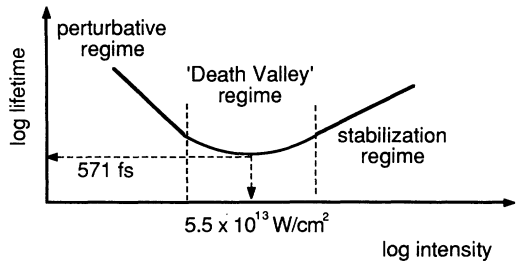

FIG. 2. Typical plot of lifetime versus intensity. The curve can be divided into three parts. At low intensities the curve follows perturbation theory and the lifetime is linear in the inverse intensity. At the highest intensities the lifetime actually increases with intensity. For intermediate intensities there is a critical intensity for which there is a minimum lifetime. The two values along the axes correspond to the calculated values [20] for the $5g$ state in hydrogen.

The minimum lifetime is somewhat larger (a factor of 3 [20]) than the time obtained by extrapolating the perturbative part of the curve to the critical intensity. To enhance the minimum lifetime, one should have a state that stabilizes easily (low critical intensity) and has a small perturbative cross section. Both the critical intensity and the cross section depend on the wavelength of the stabilizing pulse. In our experiment the choice of wavelength was dictated by the availability of short (100 fs), intense pulses at 620 nm.

D. Stabilizing properties of circular Rydberg states

It is possible to estimate the intensity at which Death Valley occurs. At that intensity there will already be a significant deviation from Fermi's "golden rule." From an intuitive picture this critical intensity corresponds to a quiver amplitude α_0, roughly the size of the initial Rydberg state n^2:

$$\alpha_0=\sqrt{I}/\omega^2=n^2 . \tag{2}$$

In this formula I is the intensity and ω is the photon frequency, in atomic units. If $\alpha_0 \ll n^2$, then the quiver motion of the nucleus is only a slight perturbation to the state.

The result we obtain from this intuitive picture can be substantially improved by taking into account the spatial part of the wave function which actually causes most of the ionization. Muller and van Linden van den Heuvell recently showed [12] that photoionization by an optical photon (2.7 eV) is localized near the core (radius $<5a_0$), irrespective of the details of the wave function. We ex-

pect nonperturbative behavior once the quiver amplitude α_0 becomes as large as the size of this region.

These intuitive ideas are in agreement with quantitative results obtained by Potvliege and Smith [20], who recently calculated ionization rates and stabilizing intensities for the $4f$, $5g$, and $6h$ circular states in hydrogen. The minimum lifetimes are 48, 571 and 8400 fs, respectively. The minimum duration of our probe laser pulses is 100 fs which means that the $4f$ state will not survive Death Valley. Although we did manage to excite h states in xenon [22], the overlap with the core and therefore the excitation probability is almost negligible, due to the high angular momentum of this state. The $5g$ states thus seem to be the best compromise.

E. Excitation of a circular state

A convenient way of exciting circular Rydberg states of moderate angular momentum l is to use a circularly polarized pump beam. The angular momentum of the excited state depends on the number of photons absorbed in the excitation. For excitation of hydrogen or helium, where the ground state is an s state, the angular momentum would be equal to the number of circularly polarized photons needed for excitation. Other noble-gas atoms have a ground-state configuration containing a closed p subshell for the most loosely bound electrons. For excitation with N photons, the lowest accessible angular momentum is $l=N-1$ if excitation starts in the $m=-1$, p orbital of the ground state.

F. Suitability of the 5g state

From the various calculations and the intuitive picture given above, it follows that we can satisfy the three conditions required for stabilization simultaneously by using the $5g$ state: First, the energy of the laser photons is high compared to the binding energy of the Rydberg state (2 eV >0.544 eV). Second, the pulse duration is shorter than the minimum lifetime (100 fs <572 fs). Third, the critical intensity, 5.5×10^{13} W/cm^2, is experimentally accessible.

Higher-lying circular Rydberg states would have even longer minimum lifetimes. However, they were not an attractive option for our experiment since such states are so closely spaced to their neighbors that the ionizing pulse, with a typical bandwidth of 16 meV, could also populate neighboring states. In that case, even if stabilization was seen, it would still be difficult to rule out that a transient mechanism, as discussed in Sec. II C, was causing the stabilization.

G. Considerations concerning the atomic species

Although the calculations have been performed for Rydberg states of atomic hydrogen, we expect that the precise atomic species is not important since the circular states we use have high angular momentum and, therefore little, interaction with the core. The small interaction manifests itself in the almost-zero quantum defects.

A problem that limits the maximum intensity that can be used in the experiment is the abundant presence of ground-state atoms. Since in practice it seems impossible to excite 100% of all the ground-state atoms to the desired Rydberg state, ionization of the atoms still in the ground state can cause a severe background signal. Thus the ground state of the atom should not be ionized by the laser intensity necessary for stabilization. Only atoms with a large ionization potential allow the use of the required high intensities.

After some preliminary experiments on xenon and argon and in accordance with appearance intensities measured by Mevel *et al.* [23], we concluded that only neon and helium would withstand sufficiently high intensities to reach the stabilization regime. The actual experiment was carried out in neon since the required wavelength (≈210 nm) to excite the $5g$ state in helium (a four-photon process) was prohibitively difficult to produce.

Like circular Rydberg states, alkali-metal atoms also have a small ionization potential. Since this allows the use of photons with lower frequencies, the critical intensity will be much lower than for ground-state atomic hydrogen: Low-frequency photons imply high quiver amplitudes at relatively low intensities. As an alternative to using Rydberg states, we considered using the ground state of an alkali-metal atom.

However, the s ground state of an alkali-metal atom is usually strongly coupled to the continuum so that no atoms would survive Death Valley. This problem could be partly circumvented by selecting a light frequency coinciding with the Cooper minimum [24]. It is not clear that the resulting suppression of ionization would persist into the high-intensity regime, where ac Stark shifts and multiphoton processes play an important role. Furthermore, even in the perturbative regime, the Cooper minimum is often not very deep, as a result of spin-orbit coupling. It is also favorable to use a state that can be selectively prepared in a small volume, rather than using a ground-state atom that homogeneously fills the laser focus, as will be explained in Sec. IV A.

IV. EXPERIMENTAL CONSIDERATIONS

A. The advantage of a pump-probe experiment

When performing high-intensity experiments, there is always a range of peak intensities in the focal region. For obtaining intensity-resolved results, this requires deconvolution of the measured data. Especially for observing stabilization, this could be a serious difficulty: Even if the stabilization regime could be reached at some point in the focus, there may still be an increased yield from the outer parts of the focus. To detect a decreasing yield from this much smaller inner focal region amid the increasing signal is close to impossible.

To overcome this difficulty, we chose to prepare states only in a small focal region using a tightly focused pump-laser pulse. We subsequently study the single-photon ionization rate due to a problem laser with an overlapping, much larger focus. This is sketched in Fig. 3. The peak intensity of the probe laser is almost constant over the pump-laser focus.

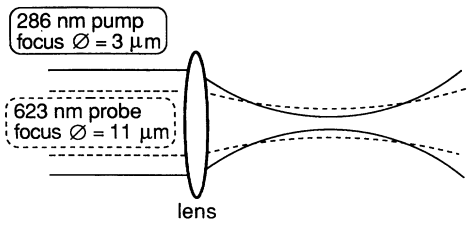

FIG. 3. Overlapping laser foci. The confocal parameter is much longer than the focus diameter. The pump laser wavelength (286 nm) is shorter than that of the probe (620 nm), and in addition it has a smaller f number so that its diffraction-limited spot diameter is smaller.

In Fig. 4 the three stages of the experiment are shown schematically. They will be discussed in more detail in Secs. IV B and IV C.

B. Larmor precession of the wave function

With a circularly polarized laser beam we excite circular wave functions with rotational symmetry along the direction of the pump laser. As discussed previously, theory predicts that stabilization will occur most readily for a circular state, if the laser polarization is along this symmetry axis, since then the quiver motion will increase the average distance of the electron to the nucleus. The linearly polarized probe beam should therefore be oriented so that its polarization is along the propagation direction of the pump beam. The most straightforward way to achieve this is to orient the beams at right angles with respect to each other. However, since the confocal parameter is longer than the focus diameter, the beam directions should be parallel to achieve acceptable overlap of the ellipsoidal foci.

This problem was solved using the 0.9-T magnetic field present in the interaction region in our electron spectrometer [25]. In this magnetic field the wave function will undergo a Larmor precession. After approximately 20 ps (a quarter Larmor period), the symmetry axis will have rotated 90° and the probe beam can be sent in with its polarization along this axis.

The 5g state in neon is very much like that in hydrogen, as can be deduced from the near-zero quantum defect. The most important difference for the current experiment is the coupling between the various angular momenta present in the atom. The coupling scheme in singly excited states of noble gases is best described in terms of so-called jK coupling [26]. In this scheme the spin $\mathbf{s}_1$ and orbital angular momentum l_1 of the valence-shell hole created by the excitation are coupled first, to form the "core" angular momentum $\mathbf{J}_{\text{core}}$. The latter then couples with the orbital angular momentum l_2 of the excited electron, to form an angular momentum $\mathbf{K}$, both by the electric-quadrupole interaction and magnetic-dipole interaction between the charge distributions. Finally, $\mathbf{K}$ couples with the spin $\mathbf{s}_2$ of the excited electron to form the total angular momentum $\mathbf{J}$, mainly by spin-orbit interaction.

The coupling of $\mathbf{s}_2$ with the other angular momenta is extremely weak in a g state. In hydrogen it amounts to only 0.0024 cm^{-1} [27], and although no experimental data are available that resolves the splitting in neon, the splitting is expected to be the same as in hydrogen. In our experiment, the 0.9-T magnetic field causes a Zeeman splitting of 0.4 cm^{-1}. Thus, with respect to $\mathbf{s}_2$, we are in the strong-field limit of the Paschen-Back effect [26], where $\mathbf{s}_2$ is completely decoupled and therefore can be ignored. The other couplings (4 and 781 cm^{-1}), however, are still large with respect to the Zeeman splitting, and cause exchange of angular momenta between the degrees of freedom l_1, l_2, and $\mathbf{s}_1$. We assume that the 0.9-T magnetic field is weak enough to safely ignore the off-diagonal elements of this perturbation, so that the Zeeman splitting can be obtained from the g factors of the eigenstates resulting from the coupling of these three angular momenta. The eigenstates of neon in the jK coupling scheme in terms of the uncoupled eigenstates $|m_l m_{s_1} m_2\rangle$ are given in Table I.

The five-photon excitation couples the ground state

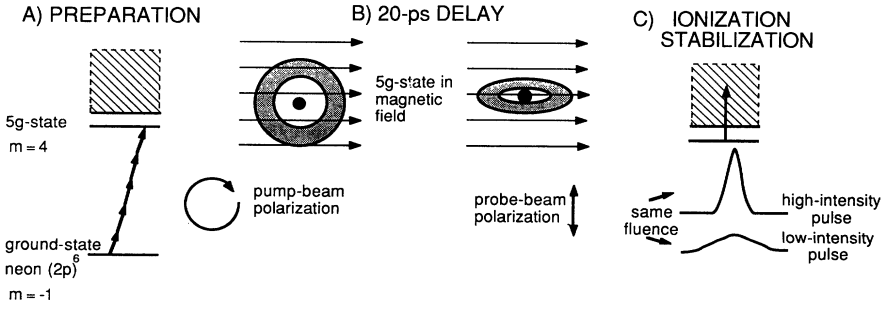

FIG. 4. Experimental scheme: (A) A pump pulse excites the 5g circular ($m = 4$) state in neon. (B) We allow the atomic wave function to rotate due to a magnetic field (this is called Larmor precession) until the atom is circular with respect to the vertical polarization of the probe laser. (C) Subsequently, the photoionization yield is measured using high- and low-intensity pulses of the same fluence.

TABLE I. Eigenfunctions with $|J|=5$ of $(2p)^{-1}(5g)$ in the jK coupling scheme, in terms of the uncoupled states $|m_1 m_{s_1} m_2\rangle$. The relative excitation probabilities are also given.

State	m_K	g factor	Wave function	Relative experimental probability
$P_{3/2[11/2]}$	11/2	12/11	$\|11/24\rangle$	50%
$P_{3/2[11/2]}$	9/2	12/11	$(\sqrt{2}\|01/24\rangle+\|1-1/24\rangle+\sqrt{8}\|11/23\rangle)/\sqrt{11}$	4.5%
$P_{3/2[9/2]}$	9/2	314/297	$4\|01/24\rangle+\sqrt{8}\|1-1/24\rangle-3\|11/23\rangle)/\sqrt{33}$	12%
$P_{1/2[9/2]}$	9/2	26/27	$(\|1/24\rangle-\sqrt{2}\|1-1/24\rangle)/\sqrt{3}$	33%

only to states with a total orbital momentum $m_1+m_2=5$, i.e., $|1\,\frac{1}{2}4\rangle$ and $|1-\frac{1}{2}4\rangle$. Thus the coefficients of these uncoupled states squared give the relative probabilities for excitation (see Table I).

In neon the spin-orbit coupling of the core is 97 meV, much larger than the bandwidth of the exciting laser. Ordinarily, this means that the selectivity of the excitation is large enough to excite only one particular eigenstate of $\mathbf{J}_{\text{core}}$ (either the $P_{1/2}$ or the $P_{3/2}$ state). In this case, however, the ac Stark shifts are so large (>1 eV) that both these states are shifted into resonance, although at different times during the pulse. Since there is no definite phase relation between the two excitations, it is most useful to think of the excited state as an incoherent superposition of states with $\mathbf{J}_{\text{core}}$ values equal to $\frac{1}{2}$ and $\frac{3}{2}$.

The other states are split much less than the laser bandwidth, but more than the Zeeman splitting caused by the 0.9-T magnetic field. This means that they will be excited as a coherent superposition (or wave packet) and that the exchange of angular momenta (the evolution of the wave packet) will take place on a time scale shorter than the Larmor period. Without magnetic field, the largest contribution of the $5g$ ($m=3$) state would occur if all $|1\,\frac{1}{2}3\rangle$ components were in phase. At that time the wave packet would have 13% $5g$ ($m=3$) character. This contribution seemed small enough to ignore in the interpretation of our experiments.

A potentially larger problem is the difference in g factors. This difference causes the states to precess at a different rate. So even if all the states would retain their pure $5g$ ($m=4$) character with respect to the precessing quantization axis, the axes would not coincide after some time. The description of the states with respect to any axis would thus contain lower m components.

Fortunately, the g factors are all very close to 1, reflecting the large contribution of orbital angular momentum with respect to spin. Thus the dephasing only occurs after many Larmor periods. This behavior was verified experimentally by measuring the ionization yield as a function of pump-probe delay (see Sec. VI C). The spin of the excited electron, of course, precesses at twice the Larmor frequency, but this does not affect the ionization yield in any way.

C. Observing deviations from Fermi's "golden rule"

According to Fermi's "golden rule", the yield for single-phonon ionization should be independent of pulse duration as long as the fluence (time-integrated intensity) remains the same. A smaller yield due to pulses with higher peak intensity would indicate that Fermi's "golden rule" no longer holds and that the stabilization regime was reached. The pulse duration was varied by chirping the pulse, which disperses the various frequency components.

Chirping changes the instantaneous frequency within the pulse duration, while the bandwidth of the pulses remains the same. An alternative would have been to decrease the bandwidth of the pulses being amplified. In that way we would have obtained longer bandwidth-limited pulses. Unfortunately, decreasing the bandwidth implies throwing away pulse energy in the frequency-selection process. This loss was not sufficiently compensated in the reamplification, so that a fluence similar to that in the short pulses would have not have been obtained.

Therefore we used the technique of chirping the pulses. By keeping the bandwidth constant, the amplification process was not changed much and approximately the same pulse energy was obtained after reamplification. There is no theoretical reason to expect the chirp to make a difference for single-photon ionization in the perturbative regime. The stabilizing regime was only reached for short, chirp-free pulses.

V. EXCITATION STEP

A. Technique

The first step of the experiment was the production of $5g$ states in neon. A problem with g states is that their ionization cross sections are so small that they ordinarily do not give rise to a recognizable peak in the electron spectrum due to multiphoton ionization, even if they are excited [22]. Therefore we used a recently introduced technique [28] of first exciting the $5g$ state with a pump laser and subsequently performing the ionization with a second laser pulse with a much larger fluence in a nanosecond pulse. The pump laser is sufficiently short and intense to drive the five-photon excitation process. The second laser subsequently saturates the single-photon ionization step.

B. Experimental setup

Our setup includes a colliding-pulse mode-locked dye laser (CPM), amplified at 10 Hz in four Bethune-type dye

cells. After recompression in a folded four-prism sequence, we obtain 100-μJ, subpicosecond pulses at 620 nm [29]. Part of the resulting beam is used for continuum generation in a water cell. For this experiment we selected a 3-nm-wide part of the white-light continuum around 571.5 nm with a grating-based pulse-shaping device [30,29]. Such a bandwidth corresponds to a pulse duration of about 330 fs. The selected light was amplified in five dye cells (diameters 1, 1, 3, 8, and 16 mm) up to an energy of 1.5 mJ. The dye we used was rhodamine 590 (6G). The resulting pulses were collimated down to 8 mm and frequency doubled in a 4-mm-long potassium diphosphate (KDP) crystal to obtain up to 200 μJ of 286-nm ultraviolet light in an approximately 1-ps-long pulse. The remaining light at the fundamental frequency was filtered out using a harmonic separator, transmitting at 600 nm and reflecting at 300 nm for an incident angle of 45°. The beam splitter was turned to optimum transmission of the fundamental frequency.

Initially we maximized the excitation process. For that purpose we used a small fraction of the Nd:YAG (yttrium aluminum garnet) beam, pumping the dye cells, as a saturating probe laser (532 nm, 5-ns pulses). The peak of the probe arrives about 2 ns after the pump laser. The energy of the probe laser was reduced to approximately 2 mJ, by reducing the size of an aperture in the beam until the probe laser caused no ionization by itself.

The two beams are combined using a harmonic separator, which was identical to the one used to filter out the fundamental frequency from the pump beam. Since the harmonic separator essentially only reflected the vertical polarization component of the pump beam, the only way to make the pump beam circularly polarized was by putting a quarter-wave plate after the harmonic separator. The quarter-wave plate was designed for 313 nm, but could be angle tuned to operate at 286 nm. The quarter-wave plate also changed the polarization of the probe beam, but this was not important since the probe fluence was sufficiently high to saturate the photoionization for any polarization.

Spatial overlap of the laser foci was obtained by propagating the beams before the focusing lens over a distance of several meters to ensure that the beam directions were the same. The probe beam was made slightly convergent by using a 1-m lens. Both beams were then focused into the spectrometer using a fused silica lens ($f=50$ mm). At this point the beam diameters were 6 and 3.5 mm, for the pump (286 nm) and probe (620 nm) beams, respectively. Due to chromatic aberration, the probe beam would normally focus 3 mm behind the pump focus. As a result of the extra 1-m lens, this distance was reduced to 0.4 mm. The probe-beam diameter at the pump focus position can be calculated geometrically, and was 50 μm. This results in a fluence of 100 J/cm^2, which was sufficient to ionize virtually all the excited-state population.

The electron spectrometer is of the magnetic-bottle type, containing a magnetic field of about 0.9 T. It is an improved version of the original Kruit and Read spectrometer [25]. The spectrometer has a background pressure of 5×10^{-9} mbar. During this experiment studying the excitation, the ionization chamber was filled with 1×10^{-4} mbar of neon. At the resulting signal level, the resolution of the spectrometer is determined by space charge in the laser focus, which reduces the spectrometer resolution to approximately 50 meV.

C. Maximizing the excitation process

The preparation of the 5g state requires the absorption of five circularly polarized photons. By varying the wavelength, we can choose the intensity at which the five-photon transition to the 5g state shifts into resonance [31]. In this way we optimized the amount of population in the 5g state. If the zero-intensity detuning is small, the resonant intensity is low. As a consequence, the five-photon excitation rate is also very low and only a small fraction of population is transferred. It is therefore advantageous to increase the zero-intensity detuning. If the detuning becomes too large, there are two problems: In the first place, five-photon ionization can occur at lower intensities, before the 5g state is shifted into resonance. This would deplete the ground state and the resulting electron signal would overwhelm the spectra. In the second place, the large intensity required to shift the state into resonance implies a high fluence, which would all ready ionize the state during the excitation pulse.

The pulse duration was determined by the length of the doubling crystal [32]. The longer the crystal, the narrower the bandwidth of the doubled pulses. In principle, we could attempt to obtain 100-fs doubled pulses. However, the required crystal length is then so short (≈0.5 mm) that hardly any light is doubled. In addition, a short pulse implies a short resonance time, which limits the population transfer. Experimentally we endeavored to find the best tradeoff between short pulse duration for maximum intensity and a long crystal for high doubling efficiency and a long resonance time.

Our optimum result was obtained when we used 286-nm, 1-ps pulses, after doubling in a 4-mm-long KDP crystal. At an intensity of $8.6\times10^{13+}$ W/cm^2, the 5g state shifts into resonance and is populated. The circular 5g state is accessed with a $\Delta m=+5$ transition from the $m=-1$ orbital in the p ground state. At this wavelength the higher-lying g states shift through resonance at lower intensities and are also populated.

In principle, the i series is also accessible, starting from the $m=1$ orbital, but the matrix element to states with such higher angular momentum is very small [22] and, furthermore, such states only exist for $n>6$. The use of circularly polarized light forbids transitions to d states, since they have no $m=4$ sublevel, but a slight contamination of the beam with linear polarization would allow such a transition.

D. Experimental results

In Fig. 5(a) the electron spectrum due to the pump laser only is shown. The width of the nonresonant broad structure corresponds to a 2-eV maximum shift of the ionization potential and therefore to a maximum intensity of about 26×10^{13} W/cm^2. When the probe laser is also present [Fig. 5(b)], we see the signal corresponding to

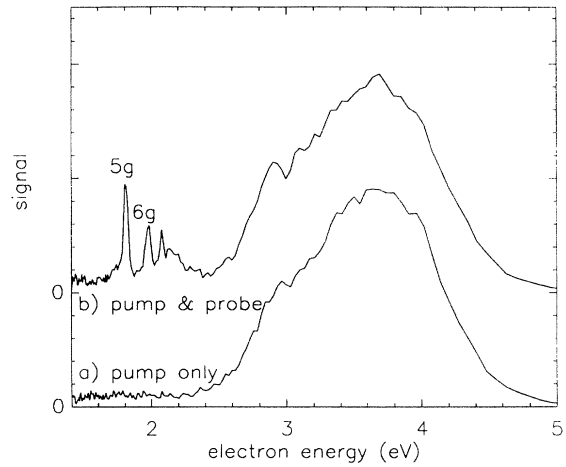

FIG. 5. (a) Electron energy spectrum of neon ionized with pump pulses only (1 ps, 286 nm, circularly polarized). The broad bump at 3.6 eV corresponds to six-photon ionization via off-resonant continuum g states. (b) When the probe pulse (5 ns, 532 nm) arrives 2 ns after the pump pulse, well-resolved additional peaks are seen. They correspond to excitation of Rydberg g states by the pump beam and subsequent one-photon ionization by the probe laser.

ionization of the $5g$ to $10g$ states. For the pulse duration of 1 ps, the saturation fluence for photonization of the $5g$ state by the pump laser, 395 J/cm^2, corresponds to an intensity of 40×10^{13} W/cm^2. This intensity is never reached so that almost all the excited population survives the pump pulse. The energies of the peaks in the electron spectrum corresponds to the energy of one probe photon (2.33 eV) minus their binding energy ($1/2n^2$, in atomic units). The binding energies of the most prominent g states are given in Table II.

For the $5g$ state and the wavelength of the probe, the saturation fluence is $\approx$40 J/cm^2 [20]. In a 5-ns pulse, this corresponds to an intensity of 8×10^9 W/cm^2 and a negligible ponderomotive shift of 0.2 meV. Since the ionization takes place on a nanosecond time scale, the lifetime is so long that the peaks are not appreciably lifetime broadened.

In accordance with a previous experiment [22], we attribute the large bump around 4 eV in the electron spectrum to nonresonant ionization via the *g continuum*. After absorption of five photons, the angular momentum is necessarily large ($l\geq4$) and the centrifugal force prevents the wave function from penetrating near the core. In consequence, the ionization cross section of the *bound g* states is so small that they have negligible contribution to the ionization signal.

From this preliminary experiment, and especially Fig. 5, we concluded that it was indeed possible to excite $5g$ states using circularly polarized light. The $6g$, $7g$, etc. states are also populated significantly. However, the total electron yield is dominated by nonresonant ionization via continuum states.

VI. THE STABILIZATION EXPERIMENT

A. Experimental setup

After having shown the feasibility of preparing circular $5g$ states, these states could be used as initial states in an experiment to demonstrate stabilization. The electron spectrometer and the circularly polarized pump beam (286 nm, 1 ps) are the same as described in Sec. V. Figure 6 is a sketch of the complete setup. The neon pressure in the spectrometer was increased to 3×10^{-4} mbar. For the stabilization experiment we used a different probe beam. A part of the amplified CPM pulses was sent through a pulse shaper [30,29] to adjust the frequency chirp (see Fig. 7). Using this device, the pulse duration could be adjusted to be as short as 0.1 ps or as long as 3

TABLE II. Some relevant parameters of the g states. The state designation is given along with the binding energy. The intensity at which the state shifts into resonance of 286 nm is given. In addition, the saturation fluence for the applicable wavelengths and polarizations are given. The saturation fluence for the complete manifold of m sublevels is only given for the $5g$ state, since the other manifolds scale in the same way.

State n,l,m	E_{bind} (eV)	I_{res} (W/cm^2)	λ (nm)	Polarization	F_{sat} (J/cm^2)
5 4 4	0.544	86×10^{12}	286	Circular	395
5 4 4	0.544	86×10^{12}	532	Linear	39
5 4 4	0.544	86×10^{12}	620	Linear	14.9
5 4 3	0.544	86×10^{12}	620	Linear	8.3
5 4 2	0.544	86×10^{12}	620	Linear	6.4
5 4 1	0.544	86×10^{12}	620	Linear	5.6
5 4 0	0.544	86×10^{12}	620	Linear	5.3
6 4 4	0.378	64×10^{12}	286	Circular	401
6 4 4	0.378	64×10^{12}	532	Linear	43
6 4 4	0.378	64×10^{12}	620	Linear	17
7 4 4	0.278	51×10^{12}	286	Circular	507
7 4 4	0.278	51×10^{12}	532	Linear	53
7 4 4	0.278	51×10^{12}	620	Linear	22

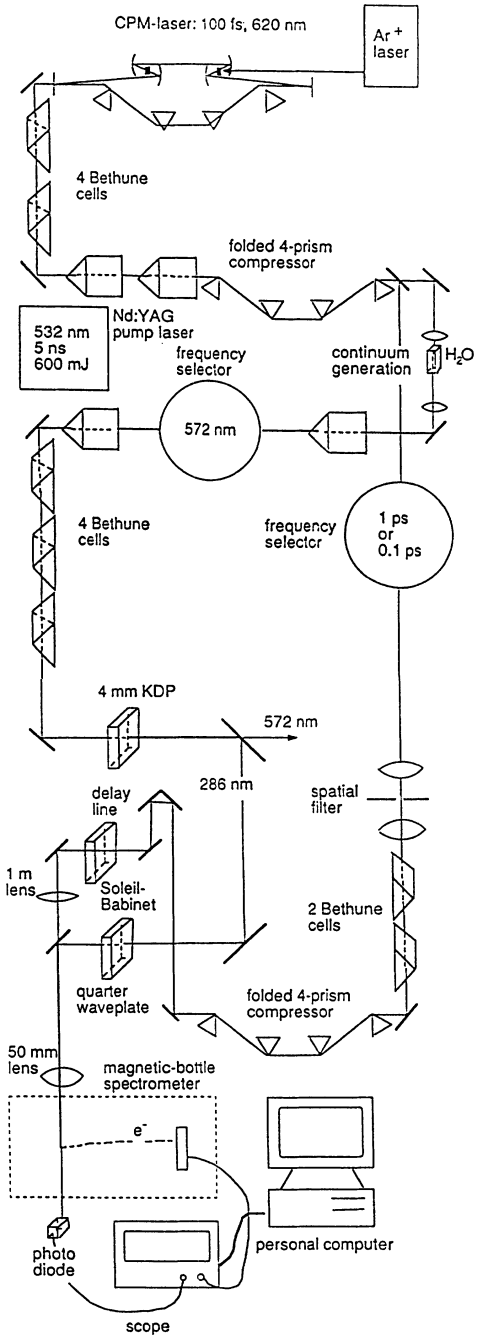

FIG. 6. Experimental setup: Shown are the CPM laser, initial amplification, and recompression. Then the 620-nm beam is split into a pump and a probe beam. Pump: following continuum generation, a 3-nm broadband around 572 nm is selected, reamplified, and frequency doubled. The 286-nm light is subsequently made circular and focused into the spectrometer. Probe: The 620-nm light travels through the shaper where it can be chirped out to 3 ps. Subsequently, it is spatially filtered and reamplified. A 1-m lens allows the focus to be accurately overlapped with that of the pump inside the magnetic-bottle spectrometer.

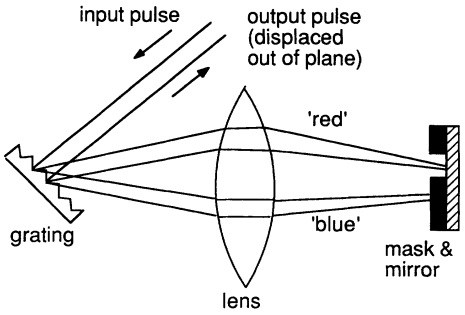

FIG. 7. Sketch of the shaper. The input beam is diffracted off a grating and forms a spectrally resolved line focus on the mirror. The reflected beam is displaced out of the plane of the Figure and recombined on the same grating. The distance from grating to the lens determines the chirp of the output pulse.

ps. The bandwidth of the resulting pulse was measured to be 5 nm around 623 nm.

After the sharper, apertures could be put into the beam to vary the final pulse energy and, as a consequence, the maximum fluence in the focus. A change in beam direction or profile due to possible misalignment in the pulse shaper or the influence of the apertures was prevented from propagating through the system by subsequent spatial filtering to the diffraction limit.

After the spatial filter, the pulses were reamplified in two dye cells (diameters 3 and 8 mm) and recompressed once more in a folded four-prism sequence. Recompression was necessary, since it was impossible to precompensate for the dispersion in the amplifier chain, due to self-phase modulation in the dye cells if the pulse is short at the output. An aperture was used to select the 5-mm-wide center of the beam, containing up to 55-μJ energy per pulse.

The two beams were combined using the same harmonics separator as before,wand were subsequently sent through the quarter-wave plate. The change of polarization of the probe beam was precompensated by adding a Soleil-Babinet compensator in the probe beam. The compensator was adjusted so that the probe polarization after the quarter-wave plate was vertical, i.e., perpendicular to the magnetic field.

The timing of the probe pulses with respect to the pump pulses could be adjusted using a computer-controlled delay line. It was checked that changing the delay between the two pulses did not vary the spatial overlap between the two foci. We now used the 1-m lens in the probe beam to precisely adjust the probe focus position to spatially overlap the pump focus. We monitored the fluence of the probe beam by measuring the pulse energy, behind the electron spectrometer, with a photodiode.

B. Focus size determination

Our setup allowed us to measure the size of the probe focus, in the way that Normand *et al.* [33] described. We

measured the magnitude of the 5*g* overlap peak, due to the presence of both beams, when the probe arrives 40 ps after the pump. We made sure that the fluence of the red beam did not saturate the ionization. We then used the 1-m lens in the probe beam to scan the relative position of the two foci in three dimensions. This gives us a measure for the red probe intensity at the pump focus. The result, shown in Fig. 8, was consistent with a diffraction-limited probe focus diameter of 11 μm (full width at half maximum) and a pump focus that was significantly smaller (≈ 3 μm). Thus all prepared Rydberg states essentially see the same peak intensity of the red pulse.

In the pump focus, at a pressure of 3×10^{-4} mbar, there are approximately 1700 atoms. Since we detect approximately 50 electrons per laser shot in the entire electron spectrum and our detection efficiency is approximately 25%, this means that the depletion of ground-state atoms is about 12%. On average, the pump pulse excites about one atom per shot to the 5*g* state.

A disadvantage of having a large probe focus is the large amount of signal due to the probe only. Ground-state depletion by the red is, however, completely negligible even at the highest intensities studied. For the background measurement it is important to remember that the volume of the probe focus is two orders of magnitude ($(\frac{11}{3})^4$) larger than the pump focus. Even if the pump pulses would significantly deplete the number of ground-state atoms, this would hardly affect the background signal due to the probe beam.

C. Photoionization yield as a function of delay

To determine the Larmor precession of the excited state, we measured the photoionization yield as a function of the delay between pump and probe. For constant fluence and for the shortest possible pulses, the result is given in Fig. 9. There is a variation of the ionization cross section as the amount of population in the various m sublevels changes. The cross sections of the various m states are given in Table II. The $1/e$ saturation fluences are calculated as

$$F_{\rm sat}=\frac{2}{\pi}\frac{1}{\Phi^2 M^2}\ . \tag{3}$$

The radial part of the overlap integral,

$$M^2=|\langle f|\varepsilon r|i\rangle|^2\ , \tag{4}$$

is calculated using a computer code for hydrogenic wave functions. From this it turns out that ionization to the h continuum dominates.

The angular part of the overlap integral is for linear polarization [34]:

$$\Phi^2=\frac{(l+1)^2-m^2}{(2l+3)(2l+1)}\ . \tag{5}$$

In this formula, l is the angular momentum of the initial state, i.e., 4. The magnetic quantum number m is the same for the initial and final states. To describe the excitation using circularly polarized light, it is easiest to use the beam direction as quantization axis. After excitation, the quantization axis will be along the magnetic-field direction, however. The relative amounts of population in the various sublevels after excitation as a function of time can be straightforwardly calculated [35] by using a rotation matrix. For this calculation we neglect spin-orbit and other angular couplings and assume that initially only the $m=4$ state is populated.

After 0, $\frac{1}{2}$, etc., Larmor periods, the states with high quantum number m are hardly populated. In the $m=\pm4$

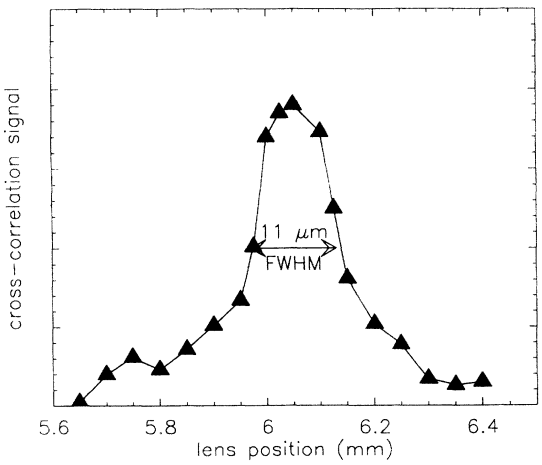

FIG. 8. Scan of the probe-focus intensity. By translating the 1-m lens, we vary the position of the probe focus relative to the pump focus. The measured signal is a good measure for the probe fluence at the position of the much smaller pump focus.

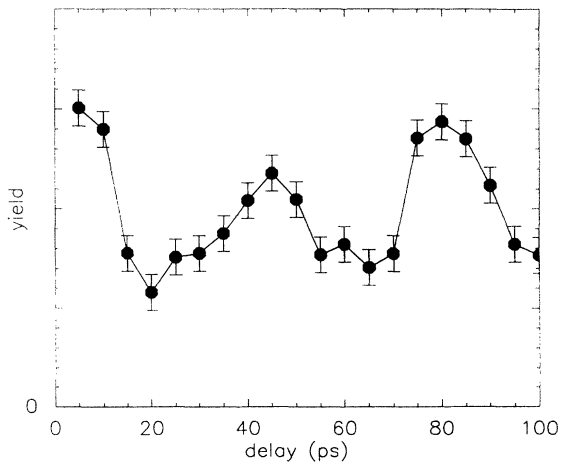

FIG. 9. Photoionization yield of the 5*g* circular state as a function of delay between pump and probe pulse. The probe pulse was short (0.1 ps) and the peak intensity was high (12×10^{13} W/cm^2). The variation of yield reflects the varying amounts of population in the different m sublevels of the 5*g* state. At $t=20$ ps (60 ps, 100 ps, etc) the yield is seen to be minimal. This is expected since the state is then predominantly circular ($m=4$) and therefore difficult to photoionize.

states there is only 0.8% of the population and only another 6% is in the $m=\pm 3$ sublevels. After $\frac{1}{4}$, $\frac{3}{4}$, etc., Larmor periods, all the population will reside in the circular states ($m=\pm 4$).

Since we observe the Larmor precession in the delay scan, we can determine the Larmor period and at what delay times stabilization should be most readily observable. At $t=20$ ps, 60 ps, etc., the yield is lowest, as expected for a magnetic field of 0.9 T. These times correspond to most of the population in the circular $m=\pm 4$ states, since the cross section of these circular states is about a third ($\frac{9}{25}$) of the cross section for the $m=0$ states. The delay scan therefore tells us to look for stabilization at $t=20$ ps, 60 ps, etc. To minimize the problem of different precession rates of the various spin-orbit components, the stabilization measurements were performed at $t=20$ ps.

D. Results

With both the pump and the probe beam present, the electron spectrum shows a sequence of peaks due to the probe ionizing the g states prepared by the pump (see Figs. 10 and 11). To study the saturation behavior of the 5g states, the magnitude of the corresponding peak was measured as a function of the fluence of the probe pulse, for two different pulse durations [5]. In principle, the yield will depend on the fluence, on whether the peak intensity is hard enough to cause stabilization, and on the distribution of population over the various m states. If the stabilization regime is reached with the short pulses (intensities up to 12×10^{13} W/cm^2), then the yield should be smaller than the yield for long pulses with the same fluence. With the long pulses, the intensity remains lower (intensities up to 1.2×10^{13} W/cm^2) and stabilization is not expected.

The presented data are extracted from a series of four spectra. Initially the delay between pump and probe was

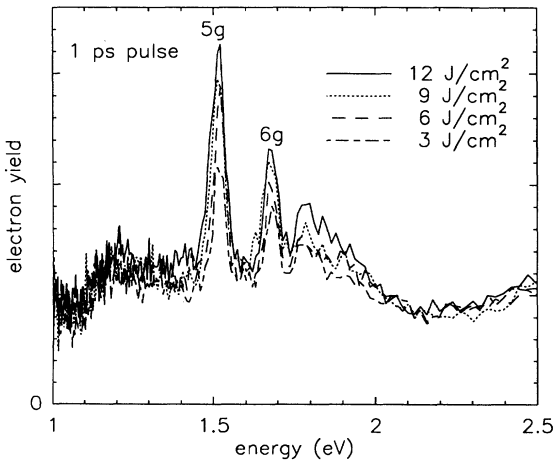

FIG. 10. Electron energy spectra for various fluences for low peak intensities, averaged over 2000 shots. The peaks at 1.5 eV correspond to one-photon ionization of the 5g state.

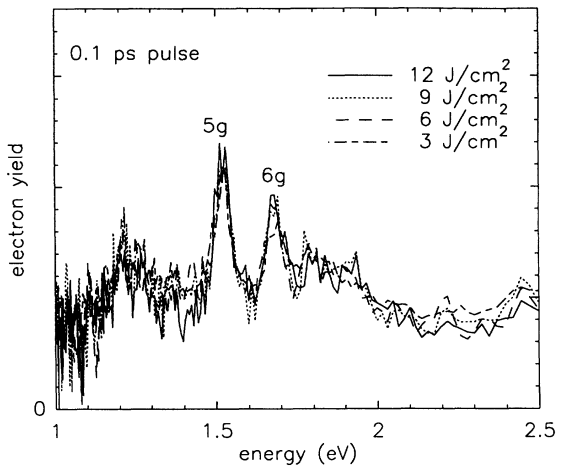

FIG. 11. Electron energy spectra for various fluences for high peak intensities. The spectra are averaged over 4000 shots. The background due to ionization by the probe pulses alone has been subtracted. The photoionization yield hardly increases with fluence.

20 ps. First, a spectrum was measured using 0.1-ps pulses with both the pump and the probe pulses present. Next, the probe pulses were chirped out to 1 ps. After adjusting the chirp with the shaper and compensating for the change in probe path length with the delay line, a spectrum was measured using the long probe pulses. Then a third spectrum was measured under similar circumstances as the first spectrum. From the deviation between the two spectra measured under the same circumstances, we could deduce the statistical error in our

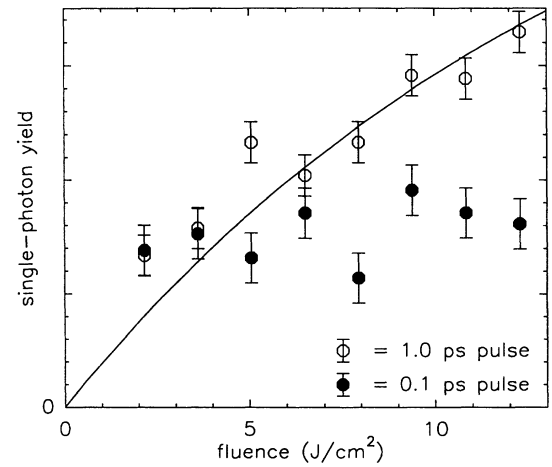

FIG. 12. Photoionization yield of the circular 5g state as a function of fluence. The open circles were measured with low peak intensity (up to 1.2×10^{13} W/cm^2, 1 ps). The curve represents a fit using the perturbative rate (including depletion) and an adjustable asymptotic value. The solid circles were measured using shorter pulses, with the same fluence but more intense (up to 12×10^{13} W/cm^2, 0.1 ps). The yield due to these pulses hardly increases with fluence, which indicates stabilization.

measurements and guard against slow drift of experimental parameters.

Finally, a further spectrum was needed: For the short pulses (0.1 ps), the probe peak intensity at the highest fluence was (12×10^{13} W/cm^2) is enough to cause some ionization of ground-state neon with the probe pulse alone [23]. Thus, before we could compare yields due to short and long pulses, some background subtraction was necessary. We obtained this background in a fourth spectrum by changing the delay to -20 ps, so that the probe arrived before the pump. For the long pulses (1 ps) no probe-only signal was present.

The short and long pulse spectra, shown in Figs. 10 and 11, have the same vertical scale. Apart from the pulse duration, the experimental circumstances and used fluences were the same. The photoionization yield of the 5*g* state, plotted in Fig. 12, was obtained by integrating a 80-meV window in the electron spectrum after subtraction of the pump-only and the probe-only signals. For the long pulses he yield still increases with fluence. For the short pulses, the peak intensities are much higher and the yield hardly increases with increasing fluence.

E. Discussion

The perturbative saturation fluence is the fluence that leaves a fraction $1/e$ of the excited population unionized. This fluence, calculated to the 15 J/cm^2 for the circular 5*g* state, was of the order of our maximum available fluence, 12 J/cm^2. Therefore, the yield, neglecting stabilization, is expected to increase with fluence. This is the case for the long pulses since no stabilization is predicted for the maximum attained peak intensity of 1.2×10^{13} W/cm^2. Figure 12 also shows a fitted perturbative curve taking into account the depletion of initial-state atoms. The asymptotic value of the curve (y axis) has been fitted but the calculated photoionization cross section (x axis) is used.

For the short pulses the peak intensities are much higher (up to 12×10^{13} W/cm^2). This intensity is higher than the theoretically predicted stabilization intensity for the 5*g* state of 5.5×10^{13} W/cm^2 [20]. In the experiment the yield hardly increases with increasing fluence. Comparison of the yields for both types of pulses therefore indicates stabilization: The single-photon ionization rate depends on the peak intensity for pulses with the same fluence.

This behavior is not caused by transient stabilization since the energy spacing from the 5*g* state to the 6*g* state is sufficiently large (167 meV) to exclude transfer of population due to the laser linewidth (16 meV). In addition, the decrease in yield cannot be caused by interference with lifetime-broadened near-lying states [13], since the spacing between the states is much larger than the width caused by the ionization rate calculated perturbatively (30 meV maximum). Therefore, the only mechanism to which we can attribute the decrease in yield is adiabatic stabilization.

As can be deduced from the delay scan (Fig. 9), the ionization yield for the "wrong" orientation of the atom (when it is mostly in an $m=0$ state) is approximately double the yield at $t=20$ ps, even with the use of the shortest pulses. Apparently, hardly any stabilization takes place for states with low values of m. Our experiments do not provide enough information to deduce if this is an intrinsic property of low-m states at the light frequency used, or if these states simply are not able to survive Death Valley becuase of the higher perturbative ionization rates.

In the spectra we also see peaks due to ionization of the higher-lying *g* states. Although the statistics for these stages is not as good, the photoionization yields from these stages, for the more intense pulses, also appear to saturate.

There is an enhancement peak in the probe-only spectra due to excitation of the 5*f* states ($m=0$) with 12 red photons, which occurs at a Stark shift of 2.86 eV. Assuming the state shifts with the quiver energy, this corresponds to an intensity of 8.0×10^{13} W/cm^2. This gives us the most accurate intensity calibration of our spectra and agrees with the measured energies, focal sizes, and pulse durations.

A possible complication is that the 5*g* population may be photoionized by two photons instead of by one photon when using the shortest, and therefore most intense, pulses. However, even for the 0.1-ps pulses, the only signal we observed due to the pump-probe combination corresponds to single-photon ionization by the probe. In Fig. 13 we show the spectrum corresponding to the difference in yield of the pump-probe combination with respect to the pump only, for the most intense probe pulses encountered (0.1 ps, $I=12\times10^{13}$ W/cm^2). The positive signal between 1.4 and 2.0 eV corresponds to single-photon ionization of the *g* states. However, there are no peaks corresponding to above-threshold ionization, which would be expected between 3.4 and 4 eV.

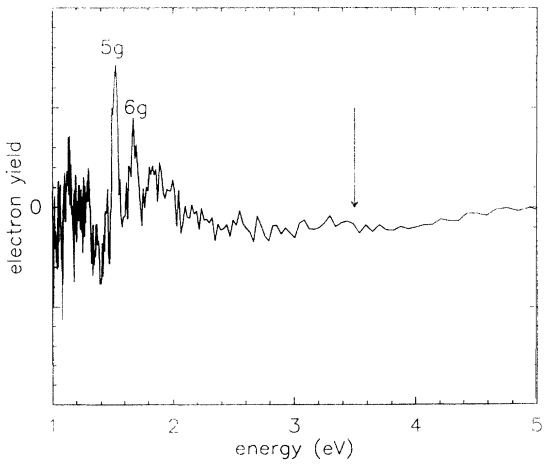

FIG. 13. Yield due to the pump-probe combination after subtraction of the pump-only signal, for the maximum intensity encountered (0.1 ps, 12×10^{13} W/cm^2). The figure clearly shows that the single-photon ionization is the only decay channel of the *g* states. The arrow indicates the expected position of the two-photon ionization signal.

TABLE III. Calculated ionization yields [36], based on [20]. The yields are for the circular $5g$ state in hydrogen ($m=4$) photoionized by 620-nm laser pulses Gaussian in time.

Fluence (J/cm^2)	Peak intensity (W/cm^2)	Pulse duration (ps)	Yield per atom
3	0.3×10^{13}	1.0	0.16
6	0.6×10^{13}	1.0	0.30
9	0.9×10^{13}	1.0	0.41
12	1.2×10^{13}	1.0	0.51
3	3.0×10^{13}	0.1	0.13
6	6.0×10^{13}	0.1	0.17
9	9.0×10^{13}	0.1	0.19

In fact, considerations from high-frequency theory predict that the single-photon ionization peak should dominate the electron spectrum, mainly because higher-order peaks require a larger momentum exchange with the nucleus. The hard collisions, required for the high-order peaks, are unlikely to occur in a circular g state, even in the perturbative regime, because the electron is localized so far from the atomic core. They are especially unlikely to occur in a stabilized state, which is localized even further from the core.

F. Comparison with theory

Our experimentally determined yields can be compared to theory since Potvliege has integrated [36] the steady-state ionization rates, calculated by Potvliege and Smith [20], for pulses of Gaussian temporal shape, that correspond to our peak intensities and pulse durations. These numbers are given in Table III. We see that indeed, for the long pulses, the yield is predicted to keep increasing and shows some saturation. For the short pulses the yield hardly increases with fluence.

Quantitatively, we can compare the yields for a fluence of 9×10^{13} W/cm^2. For the intense pulses the yield is a factor of 2 lower than the yield due to the nonstabilizing pulses. This agrees with the predictions of Smith and Potvliege who predict a factor of 2.1.

Without relying on the time-integrated results, we can also estimate the critical intensity from our data. Above the critical intensity, the ionization rate decreases with intensity. At the critical intensity, however, there will already be a significant difference in yield compared to nonstabilizing, long pulses with the same fluence. From our data we determine that this intensity is between 4×10^{13} and 9×10^{13} W/cm^2. Again, this is in good agreement with the predicted value of 5.5×10^{13} W/cm^2.

G. Outlook

A possible improvement in our experiment would be to measure the asymptotic yield, i.e., the yield due to a nonstabilizing pulse with infinite fluence. It may be possible to measure this value using an additional third beam to photoionize the atoms initially prepared by the first beam and subsequently left unionized by the second pulse. The use of such a saturating pulse (e.g. 532 nm, 5 ns) would entail combination of our preliminary experiment and the stabilization experiment. Such an experiment is currently in progress. An additional improvement would be to use longer, tailored pulses with a flat temporal profile and so allow better comparison of experimental results with theoretical results.

VII. CONCLUSIONS

A pump-probe experiment has been introduced to study the stabilization of low-lying circular states. In good agreement with calculations by Potvliege and Smith [20], we find a strong indication for stabilization of circular $5g$ states in neon at intensities above several times 10^{13} W/cm^2.

ACKNOWLEDGMENTS

This work is part of the research program of the Stichting voor Fundamenteel Onderzoek der Materie (Foundation for the Fundamental Research on Matter) and was made possible by financial support of the Nederlandse Organisatie voor Wetenschappelijk Onderzoek (Netherlands Organization for the Advancement of Research) and the European Community through Grant No. SCI-0103-C.

[1] R. R. Freeman and P. H. Bucksbaum, J. Phys. B **24**, 325 (1991).

[2] Recent theoretical overviews of intense field effects are given in K. Burnett, P. L. Knight, B. R. M. Piraux, and V. C. Reed, J. Phys. B **26**, 561 (1993); *Atoms in Intense Laser Fields*, edited by M. Gavrila (Academic, San Diego, 1992).

[3] M. Gavrila and J. Z. Kaminski, Phys. Rev. Lett. **52**, 614 (1984).

[4] M. Pont and M. Gavrila, Phys. Rev. Lett. **65**, 2362 (1990).

[5] M. P. de Boer, J. H. Hoogenraad, R. B. Vrijen, L. D.

Noordam, and H. G. Muller, Phys. Rev. Lett. **71**, 3263 (1993); H. G. Muller and M. P. de Boer, in *Proceedings of the 11th International Conference on Laser Spectroscopy (Elicols '93), June 1993, Hot Springs, Virginia* (Springer, New York, 1993/1994); H. G. Muller and M. P. de Boer, in *Proceedings of the 6th International Conference on Multiphoton Processes (ICOMP VI), June 1993, Quebec City, Canada,* edited by S. L. Chin (World Scientific, Singapore, 1993/1994).

[6] A. Einstein, Ann. Phys. (Leipzig) **17**, 132 (1905).

[7] This formula, in atomic units, is an adaptation from H. A. Bethe and R. Jackiw, *Intermediate Quantum Mechanics* (Benjamin, Reading, MA, 1964), p. 7.

[8] H. A. Kramers, *Collected Scientific Papers* (North-Holland, Amsterdam, 1956), p. 262; W. C. Henneberger, Phys. Rev. Lett. **21**, 838 (1968).

[9] L. D. Noordam, H. Stapelfeldt, D. I. Duncan, and T. F. Gallagher, Phys. Rev. Lett. **68**, 1496 (1992); K. Burnett, V. C. Reed, and P. L. Knight, *ibid.* **66**, 301 (1991); J. Parker and C. R. Stroud, Jr., Phys. Rev. A **41**, 1602 (1990); J. H. Hoogenraad, and L. D. Noordam, in *Super-Intense Laser-Atom Physics,* edited by B. R. M. Piraux, A. l'Huillier, and K. Rzążewski (Plenum, New York, 1993).

[10] J. H. Hoogenraad, R. B. Vrijen, and L. D. Noordam, Phys. Rev. A **50**, 4133 (1994).

[11] A. Giusti-Suzor and P. Zoller, Phys. Rev. A **36**, 5178 (1987).

[12] H. G. Muller and H. B. van Linden van den Heuvell, Laser Phys. **3**, 694 (1993).

[13] M. V. Fedorov and A. M. Movsesian, J. Opt. Soc. Am. B **6**, 928 (1989).

[14] Y. Gontier, N. K. Rahman, and M. Trahin, Phys. Rev. Lett. **34**, 779 (1975).

[15] H. R. Reiss, Phys. Rev. A **22**, 1786 (1980).

[16] H. G. Muller and M. P. de Boer, in *Super-Intense Laser-Atom Physics,* edited by B. R. M. Piraux, A. l'Huillier, and K. Rzazewski (Plenum, New York, 1993), Vol. III.

[17] R. R. Freeman, P. H. Bucksbaum, H. Milchberg, S. Darack, D. Schumacher, and M. Guesic, Phys. Rev. Lett. **59**, 1092 (1987).

[18] P. Marte and P. Zoller, Phys. Rev. A **43**, 1512 (1991); M. Dörr, R. M. Potvliege, D. Proulx, and R. Shakeshaft, *ibid.* **43**, 3729 (1991); K. C. Kulander, K. J. Schafer, and J. L. Krause, Phys. Rev. Lett. **66**, 2601 (1991).

[19] M. Pont and R. Shakeshaft, Phys. Rev. A **44**, 4110 (1991); R. J. Vos and M. Gavrila, Phys. Rev. Lett. **68**, 170 (1992).

[20] R. M. Potvliege and P. H. G. Smith, Phys. Rev. A **48**, 46 (1993).

[21] P. Lambropoulos, Phys. Rev. Lett. **55**, 2141 (1985).

[22] M. P. de Boer, L. D. Noordam, and H. G. Muller, Phys. Rev. A **47**, 45 (1993).

[23] E. Mevel, P. Breger, R. Trainham, G. Petite, P. Agostini, A. Migus, J. P. Chambaret, and A. Antonetti, Phys. Rev. Lett. **70**, 406 (1993).

[24] M. J. Seaton, Proc. R. Soc. London, Ser. A **208**, 418 (1951).

[25] P. Kruit and F. H. Read, J. Phys. E **16**, 313 (1983).

[26] R. D. Cowan, *The Theory of Atomic Structure and Spectra* (University of California Press, Berkeley, 1981).

[27] C. E. Moore, in *Atomic Energy Levels, Vol. 1* (U.S. GPO, Washington, D.C., 1958).

[28] M. P. de Boer and H. G. Muller, Phys. Rev. Lett. **68**, 2747 (1992).

[29] L. D. Noordam, W. Joosen, B. Broers, A. ten Wolde, A. Lagendijk, H. B. van Linden van den Heuvell, and H. G. Muller, Opt. Commun. **85**, 331 (1991).

[30] A. M. Weiner, J. P. Heritage, and E. M. Kirschner, J. Opt. Soc. Am. B **5**, 1563 (1988).

[31] P. Kruit, J. Kimman, H. G. Muller, and M. J. van der Wiel, J. Phys. (Paris) Colloq. **43**, C2-457 (1982); J. Phys. B **16**, 937 (1983).

[32] L. D. Noordam, H. J. Bakker, M. P. de Boer, and H. B. van Linden van den Heuvell, Opt. Lett. **15**, 1464 (1990).

[33] D. Normand, L.-A. Lompré, A. L'Huillier, J. Morellec, M. Ferray, J. Lavancier, G. Mainfray, and C. Manus, J. Opt. Soc. Am. B **6**, 1513 (1989).

[34] H. A. Bethe and R. Jackiw, *Intermediate Quantum Mechanics* (Benjamin, Reading, MA, 1964), p. 221.

[35] R. N. Zare, *Angular Momentum* (Wiley, New York, 1988), p. 86.

[36] R. M. Potvliege (private communication based on [20]).

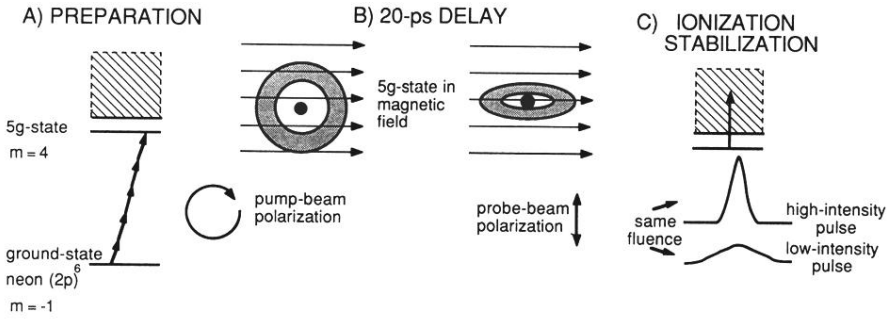

FIG. 4. Experimental scheme: (A) A pump pulse excites the 5*g* circular ($m = 4$) state in neon. (B) We allow the atomic wave function to rotate due to a magnetic field (this is called Larmor precession) until the atom is circular with respect to the vertical polarization of the probe laser. (C) Subsequently, the photoionization yield is measured using high- and low-intensity pulses of the same fluence.